Stochastic Frequency Control of Grid-connected Microgrids

Pietro Ferraro, *Student Member, IEEE*, Emanuele Crisostomi, *Senior Member, IEEE*, Robert Shorten, *Senior Member, IEEE*, and Federico Milano, *Fellow, IEEE*

***Abstract*— This paper proposes a stochastic control strategy, namely the unsynchronized Addictive Increase Multiplicative Decrease (AIMD) algorithm, to manage the power flow of interconnected microgrids (MGs). The proposed control aims at achieving a trade-off between the individual utility function of each MG while ensuring the stability of the grid. Both centralized and decentralized AIMD approaches are considered and compared. Extensive Monte Carlo simulations are performed on the IEEE 39-bus system, and show that the proposed control strategy is able to provide the sought trade-off.**

***Index Terms*— Microgrid, energy management systems, distributed energy resources, decentralized stochastic control.**

I. Introduction

Microgrids (MGs) are flexible cells operating at low voltage distribution network, composed of Distributed Energy Resources (DERs), including wind and solar plants, controllable and non-controllable loads, storage devices and possibly electric vehicles. The main feature of MGs is that they can operate both connected to the outer ac power grid and disconnected from it, i.e., in islanded mode [1], [2]. The Energy Management System (EMS) represents the intelligent core of the MG, and is responsible for choosing the "optimal" operation mode.

Initially, MGs were intended as standalone electricity supply systems in remote regions, but recent advances in generation technologies, including the increasing penetration of distributed energy resources, have raised the interest of the power community of splitting the existing power grids into semi-independent MGs [3], [4]. This approach potentially provides several advantages, e.g., it improves grid resiliency; simplifies control hierarchy; and leads to efficient decentralized regulation. Despite such promising premises, the idea of shifting from a top-down power grid to a grid of interconnected MGs is still in its infancy.

The scientific research carried out so far has mainly focused its attention on the analysis of single, often islanded, MGs. With this regard, research has mostly focused on the optimization of the scheduling of generation units and loads [5]–[7]; and the stability analysis of a MG when is switches between interconnected and islanded modes [8]–[10]. MGs also present technical challenges related to the very low rotational inertia introduced. An overview regarding the impact of the power system frequency stability has been provided in [11]. Angle and voltage stability as a function of penetration of MGs in the ac grid, is analyzed in [12] and an analytical approach to evaluate the effects of lowering the system inertia is proposed in [13].

Very few works consider the effects of the interactions among several grid-connected MGs, and the impact of the MG energy management system on the power grid. This is mainly due to the difficulty of modeling such a large-scale and high-granularity power system with the required level of accuracy. In this context, realistic simulations performed in [14] and [15] showed that a large number of MGs that opportunistically manage their power flow to optimize some individual internal utility function (e.g., revenues in selling energies) may cause large frequency deviations of the interconnecting transmission system, eventually endangering the stability of the grid as a whole. Conclusions drawn in [14] and [15] suggest the need to design appropriate control methods to maintain the power grid within safe operational boundaries as the number of MGs increases.

A possible, yet conservative solution to the problem above is proposed in [16], which considers a distributed stochastic controller to improve the security of the grid and, at the same time, allow each MG to maintain their operational freedom. The rationale for a stochastic approach, as opposed to a deterministic one, is that the latter would require heavy communication, either among the many MGs or through a centralized base station, in order to be effective. This requirement, besides the obvious economic disadvantages and robustness issues [17], might also give rise to privacy concerns [18].

When dealing with a large number of independent units, a stochastic approach ensures that, in average, the system will converge to a predetermined average behavior without the need for communication among the units. Moreover, the autonomy of each unit and the introduction of stochasticity in the control actions prevent the occurrence of harmful behaviors, such as the undesired synchronization of the control actions of the MGs, that can be harmful for the system stability [19].

Based on the models discussed in [15], [16], this paper proposes a new strategy that allows MGs to operate autonomously as much as possible, according to their individual utility functions, and, at the same time, helps reducing frequency deviations and, hence, power unbalance.

Specific contributions of this work are as follows.

- The unsynchronized Addictive Increase Multiplicative

Pietro Ferraro and Emanuele Crisostomi are with the Department of Energy, Systems, Territory and Constructions Engineering, University of Pisa, Italy. (e-mails: pietro.ferraro@unipi.it, emanuele.crisostomi@unipi.it).

Robert Shorten and Federico Milano are with the School of Electrical and Electronic Engineering of the University College Dublin, Belfield, Ireland. (e-mail: robert.shorten@ucd.ie, federico.milano@ucd.ie).

Federico Milano is funded by Science Foundation Ireland under Grant No. SFI/15/IA/3074 and by European Commission under the RESERVE Consortium (grant No. 727481).

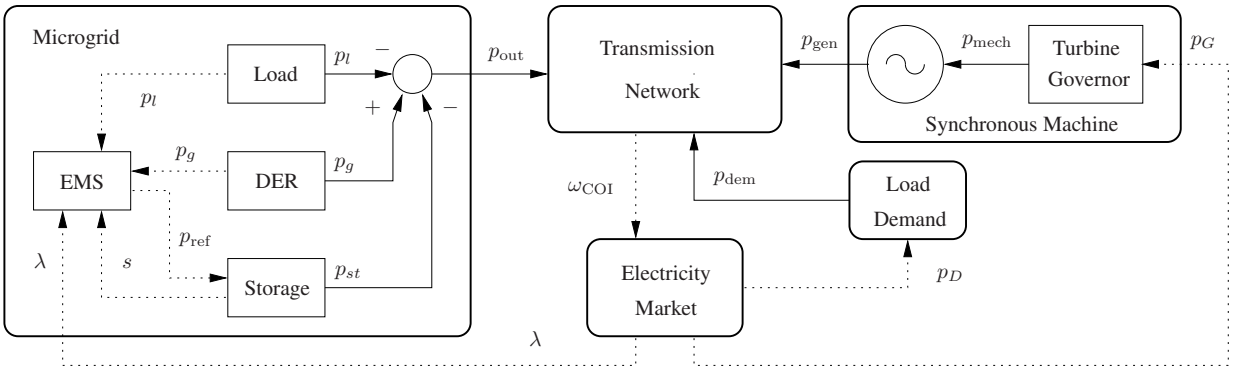

Fig. 1: Structure of the interaction between MGs, load demand, generators, the transmission network and the electricity market.

Decrease (AIMD) algorithm [18] is used for the first time in this context to mitigate the negative effects of the penetration of MGs on the frequency deviation of the transmission system.

- We compare a centralized solution of the AIMD-based strategy, where a system-wide average frequency estimation, e.g., the center of inertia, is utilized, with a completely decentralized version, where measured local bus frequencies are used instead. The comparison is performed in terms of frequency stability, fairness and operational flexibility.
- The proposed solution is shown to outperform the more conventional control strategy proposed in [16], where simple nonlinear PI-based controllers had been used to decide when MGs had to switch from a "greedy" mode to a cooperative mode.

The remainder of the paper is organized as follows. Section II illustrates the models of the power system, the electricity market, the MGs with their energy management systems, the control problem and the bus frequency estimator. Section III presents the AIMD algorithm and the proposed centralized and decentralized stochastic control schemes. Section IV discusses the case study where the proposed controls are compared. To this aim, a set of Monte Carlo stochastic time domain simulations are carried out based on the IEEE 39-bus system. Finally, main conclusions are outlined in Section V.

II. Modeling

In this paper, each MG is modeled using stochastic differential equations, taking into account loads, DERs and storage units. These elements are coordinated by an EMS which is responsible, among other tasks (e.g., load shedding, internal power flow management, transition to island mode), to establish the active power set point that the MG sells or buys from the electrical grid [3]. The following assumptions are made:

- MGs internal dynamics are, at least, one order of magnitude smaller than the ones of the high voltage transmission system [3], [20], [21]. On the basis of this consideration, their dynamics is neglected and they are treated as algebraic variables;
- Although each MG is composed of a different amount of storage units, DERs and loads, to reduce the computational burden, we used an aggregated model for all these units. This assumption can be relaxed, assuming distributed DERs, storage units and loads at the expense of a higher computational burden.

Figure 1 shows a simplified scheme that illustrates the interactions of MGs, generators and load demands with the transmission system and the electricity market. For simplicity of representation, only one MG, generator and load are represented in the figure. The remainder of this section describes the mathematical models of all the elements that compose Fig. 1 and that were implemented to carry out the simulations of the case study, namely, the power system, the electricity market, MGs, the estimation of bus frequencies, and the control problem.

A. Power System Model

The model of the power system considered in the case study is based on a set of hybrid differential algebraic equations [22], as follows:

$$\begin{aligned} \dot{\boldsymbol{x}} &= \boldsymbol{f}(\boldsymbol{x}, \boldsymbol{y}, \boldsymbol{u}) \\ \boldsymbol{0} &= \boldsymbol{g}(\boldsymbol{x}, \boldsymbol{y}, \boldsymbol{u}) \end{aligned} \tag{1}$$

where $\boldsymbol{f}$ ($\boldsymbol{f} : \mathbb{R}^{p+q+s} \mapsto \mathbb{R}^p$) are the differential equations; $\boldsymbol{g}$ ($\boldsymbol{g} : \mathbb{R}^{p+q+s} \mapsto \mathbb{R}^q$) are the algebraic equations; $\boldsymbol{x}$ ($\boldsymbol{x} \in \mathbb{R}^p$) are the state variables; $\boldsymbol{y}$ ($\boldsymbol{y} \in \mathbb{R}^q$) are the algebraic variables; and $\boldsymbol{u}$ ($\boldsymbol{u} \in \mathbb{R}^s$) are discrete events, which model the EMS logic of MGs.

The differential equations $\boldsymbol{f}$ in (1) include conventional dynamic models of synchronous machines (e.g., 6th order models), their controllers, such as, automatic voltage regulators, turbine governors, and power system stabilizers. For space limitations, we do not report here all dynamic models considered in the case study. The interested reader can find a thorough descriptions of all these models in [23].

The algebraic equations $\boldsymbol{g}$ in (1) model auxiliary variables as well as the voltage phasors and power injections of transmission network, whose lines and transformers are defined by lumped models, as follows:

$$\begin{aligned} p_h &= v_h \sum_{k \in \mathcal{B}} v_k (g_{hk} \cos\theta_{hk} + b_{hk} \sin\theta_{hk}), \quad h \in \mathcal{B} \\ q_h &= v_h \sum_{k \in \mathcal{B}} v_k (g_{hk} \sin\theta_{hk} - b_{hk} \cos\theta_{hk}), \quad h \in \mathcal{B} \end{aligned} \tag{2}$$

where $\mathcal{B}$ is the set of network buses; v_h and v_k are the voltage magnitudes at buses h and k, respectively; $\theta_{hk} = \theta_h - \theta_k$ are the differences of the voltage phase angles between bus h and k; $g_{hk} + jb_{hk}$ are the elements of the network admittance matrix [23]; and p_h and q_h are the total active and reactive power injections, respectively, at bus h.

As discussed in the remainder of this section, (1) also include market dynamics (see Subsection II-B), and the MG dynamic components, such as DERs, storage devices and loads as well as the MG energy management system and control (see Subsection II-C).

B. Electricity Market Model

In this work, it is assumed that the MGs try to maximize their revenues. The decisions of the EMS of the MGs are thus driven by the price of electricity and there is the need to properly account for the market behavior. As thoroughly discussed in [14] and [15], in fact, the market plays a prominent role in the dynamic response of the interconnected MGs. Hence, in the case study, the electricity market is modeled as in [14].

This model is based on [24], where power system dynamics are assumed to be coupled with a real-time – or *spot* – electricity market, also modeled based on differential equations. These represent an ideal market for which the energy price λ, assumed to be a continuous state variable, is computed and adjusted rapidly enough with respect to the dynamic response of the transmission system, e.g., PJM, California, etc.

For clarity, we give below the equations that describes market dynamics. The main assumptions are:

- Price variations are driven by the grid energy imbalance.
- An excess of supply decreases the price of energy while an excess of demand increases it.
- The market is ideal and that there is a single energy price.

If there are n power suppliers and m power consumers, generator and load active powers dynamics are linked to the market clearing price λ based on a dynamic version of their bidding functions, as follows [24]:

$$\begin{aligned} T_{Gi}\dot{p}_{Gi} &= \lambda - c_{Gi}p_{Gi} - b_{Gi} \\ T_{Di}\dot{p}_{Di} &= -\lambda - c_{Di}p_{Di} - b_{Di} \ , \end{aligned} \tag{3}$$

where p_{Gi} are the power orders of the n suppliers connected to the grid; p_{Dj} are the active power consumption of m loads connected to the grid; c_{Gi}, c_{Di} and b_{Gi}, b_{Di} are proportional and fixed bid coefficients, respectively, as in conventional auction models; and T_{Gi} and T_{Di} are time constants modeling generator and demand, respectively, delayed response to variations of the market clearing price λ.

The quantities p_{Gi} are the input signals to the turbine governors of the synchronous machines. The actual active power generation p_{gen} of the synchronous machines follows the dynamics of the governor, the turbine and the generator. The quantities p_{Di}, on the other hand, are the rated power consumptions imposed by the load demands, which are assumed to have a constant power factor. In Fig. 1, we have indicated the actual consumption of the loads as p_{dem}, to take into account that actual load consumptions may depend on the bus voltage magnitude [23].

The market clearing price λ is also modelled as a state variable, with a continuous dynamic, as follows:

$$T_\lambda \dot{\lambda} = K_E(1 - \omega_{\text{COI}}) - \lambda \ , \tag{4}$$

where K_E and T_λ are parameters that depend on the design of the market itself; and ω_{COI} is the frequency of the COI, defined as

$$\omega_{\text{COI}} = \frac{\sum_{i=1}^{r} H_i\omega_i}{\sum_{i=1}^{r} H_i} \ , \tag{5}$$

where ω_i and H_i are, respectively, the frequency and the moment of inertia of the i-th synchronous machine, and r is the number of conventional generators in the grid.[1]

In (4), ω_{COI} serves to define the overall power unbalance of the system. If $\omega_{\text{COI}} > 1$, in fact, the generation exceeds the demand, while if $\omega_{\text{COI}} < 1$, the demand exceeds the generation. Since the transient behavior of ω_{COI} is a consequence of the dynamic response of synchronous machines which are connected to the load through the transmission grid (see equation (2)), ω_{COI} implicitly takes into account the effect of machine regulation as well as of network losses. The interested reader can find more details on this model and its notation in [14].

C. Microgrid Model

The elements that compose the microgrid are the load, the DER, the storage device and the Energy Management System (EMS). The latter is responsible for the MG active power set point.

The dynamic of the aggregated storage device model is ruled by the following equation, which is the continuous-time equivalent of the model used in [25],

$$T_c\dot{s} \ = \ p_{st} \ = \ p_g - p_l - p_{\text{out}} \tag{6}$$

where s is the state of charge of the MG, T_c is the time constant of the storage active power controller, p_{st} is the power generated or absorbed by the storage device ($p_{st} > 0$ if the storage is charging); p_{out} is the power output of the MG; and p_g and p_l are the produced active power and the local loads, respectively, of the MG. s undergoes an anti-windup limiter that models the charged ($s = 1$) and discharged ($s = 0$) conditions.

According to the notation given in (2), at the buses where the microgrids are connected, one has:

$$p_h = p_{\text{out}} \ . \tag{7}$$

If there are other devices connected at bus h, their power injection is simply add to the right hand side of (7). Note that p_{out} is positive when the MG behaves as a generator and negative when the MG behaves as a load.

Uncertainty and volatility of both generation units and loads are accounted for by modeling the net power produced by the MG as a stochastic process according to

$$p_{\text{net}} \ = \ p_g - p_l \ = \ \bar{p}_{g_T} - \bar{p}_{l_T} + \eta_M \tag{8}$$

[1]Note that, in general, $n \neq r$ as not all power plants are equipped with synchronous machines.

where η_M is a white noise as in [28] with standard deviation σ_M, and $\bar{p}_{g_T}$ and $\bar{p}_{l_T}$ are piece-wise constant functions that account for uncertainty and change randomly with a period T as discussed in [29]. The noise is modeled as a single stochastic algebraic variable as the behavior of the MG depends on the difference $p_{\text{net}} = p_g - p_l$ and not on their absolute values. Finally, the reference set point of the active power p_{ref}, is defined by the EMS of the MG and it is imposed by the slack variable p_{st}, as shown in Figure 1. The interested reader can find a detailed discussion on the model of the MG in [14].

D. Bus Frequency Estimation

While in a practical situation the frequency can be directly measured, its estimation, in a time domain simulation based on standard transient stability models, can be a challenging task. In these models, in fact, only the frequencies (effectively, the rotor speeds) of the internal electro-motive forces (emfs) of synchronous machines are available.

To solve this issue, in this paper, we utilize the Frequency Divider (FD), which is a local frequency estimation technique proposed in [30]. The FD formula is:

$$(\mathbf{B_{BB}} + \mathbf{B_{B0}})^{-1}(\boldsymbol{\omega_B} - \mathbf{1}) = \mathbf{B_{BG}}(\boldsymbol{\omega_G} - \mathbf{1}) \qquad (9)$$

where $\mathbf{1}$, $\boldsymbol{\omega_G}$ and $\boldsymbol{\omega_B}$ are, respectively, a column vector containing 1 on each entry, the vectors of the frequencies of the synchronous machines and of the buses, while $\mathbf{B_{BB}}$, $\mathbf{B_{B0}}$ and $\mathbf{B_{BG}}$ are the imaginary part (susceptances) of the admittance matrices $\overline{\mathbf{Y}}_{\mathbf{BB}}$, $\overline{\mathbf{Y}}_{\mathbf{B0}}$ and $\overline{\mathbf{Y}}_{\mathbf{BG}}$ that represent, respectively, the standard network admittance matrix; a diagonal matrix that accounts for the internal impedances of the synchronous machines at generator buses; and the admittance matrix obtained using the internal impedances of the synchronous machines.

Equation (9) gives a simple algebraic expression between the frequencies of the synchronous machines and the buses that can be rapidly evaluated in any time domain simulation.

E. Energy Management System of the Microgrid

Extensive realistic simulation in [14] showed that MGs that only focus on their own individual convenience, e.g., the maximization of individual revenues, may lead the frequency of the grid out of a safety range. Accordingly, in this paper we propose a strategy that mitigates the impact of MGs on the power grid while at the same time allows the MGs to continue to operate advantageously according to their own policy. In particular, we achieve this result by making the MGs switch between two operating modes:

- *Market based mode* (M-Mode): The MG is free to maximize its revenues (e.g., selling and buying energy without limitations);
- *Frequency regulation mode* (F-Mode): The MG participates to the primary frequency regulation of the power grid.

In this paper, the overall goal is to allow as many MGs as possible to behave according to their own policy (the M-Mode in this case), while some of them regulate the frequency in order to reduce frequency deviations and, hence, the power unbalance of the ac grid. The M-Mode used in this paper follows the same set of *if-then* rules proposed in [14], while the F-Mode utilizes the conventional droop control equations classically employed in the primary frequency regulation of the power system [32]. Note that the two modes considered here are only two possible choices. The control strategy discussed in this paper can be applied as is to any other operating modes. Alternative operating strategies are, for example, the set of rules for the M-Mode given in [15]; and the Model Predictive Control proposed in [31] for the F-Mode.

In this paper, we control the switching between the M-Mode and the F-Mode of the i-th MG by a probability $P_{s_i}(t)$ of staying in the M-Mode. Whenever the frequency gets close to the operational boundaries of the system, then the probability $P_{s_i}(t)$ decreases and each MG switches to the F-Mode with probability $1 - P_{s_i}(t)$. Conversely, if the control signal lies within safe boundaries, each MG switches back to the M-Mode with a higher probability $P_{s_i}(t)$. Thus, the smaller is the value of $P_{s_i}(t)$ over time, the larger is the probability for the i-th MG to provide frequency regulation services. Accordingly, the goal of the i-th MG is to maximize $P_{s_i}(t)$ (i.e., keeping it as close to 1 as possible) to maximize the time spent in the M-Mode maximizing its own economic interests.

The optimization problem may be formulated as follows, where the convex, strictly differentiable functions $f_i(\cdot) : [0,1] \longmapsto \mathbb{R}$ quantify here the inconvenience of each of the n MGs to provide ancillary services to the grid:

$$\begin{aligned} \underset{\boldsymbol{P_s(t)}}{\text{minimize}} \quad & \sum_{i=1}^{n} f_i(P_{s_i}(t)) \\ \text{subject to} \quad & |\omega_i - \omega_0| \leqslant \overline{\omega}_m, \forall i \in \Theta \end{aligned} \qquad (10)$$

where $\boldsymbol{P_s(t)} \in \mathbb{R}^n$ is the vector whose i-th component is $P_{s_i}(t)$, Θ is a discrete set of indexes and $\overline{\omega}_m$ is the maximum allowed deviation from the nominal frequency, ω_0. The functions $f_i(\cdot)$ can be assigned to each MG by the System Operator responsible for the specific area (e.g., this could be based on CO_2 emissions, size of the MG, its energy class, etc).

The difficulty in solving the optimization problem (10) is due to the fact that the relationship between the controlled variables ($P_{s_i}(t)$) and the output (i.e., ω_i) is unknown. In fact, the dependency between the frequency oscillations and the operational modes of the single MGs depend on the many (time-varying) parameters of the underlying power grid, of the single MGs, and also on the (unknown) behaviors of the other MGs; and analogously, a single switching probability, or a slight change in the strategy of a single MG, affects every local frequency in the transmission system.

For this purpose, we propose the use of the AIMD algorithm to solve the optimization problem (10). The rationale of this choice is that AIMD, as outlined in greater detail in the next subsection, has the advantage of having a decentralized, model-free structure (i.e., it does not require any knowledge of the specific system it is being applied to), with very low communication requirements.

III. AIMD Algorithm

The AIMD algorithm has been widely employed in the Internet congestion control problem to optimally and fairly share bandwidth among connected users [33]. In AIMD an individual agent (e.g., a computer sending packets) gently increases its transmission rate, during the Additive Increase (AI) phase, until a packet loss signal is received. This is called a congestion event (CE), and indicates that the sum of individual bandwidths has exceeded the total capacity. Upon detecting congestion, the agents instantaneously decrease their transmission rate in a multiplicative fashion. This is the Multiplicative Decrease (MD) phase of the algorithm. Note that this algorithm does not require users to communicate among themselves, e.g., to know how many users are currently connected to the Internet.

Similarly, in this paper we assume that each MG gently increases its probability of operating in the desired M-Mode (AI phase), until it is notified of a CE (e.g., frequency close to dangerous values). Then, the $P_{s_i}(t_k^+)$ will decrease by the multiplicative factor $\beta < 1$, (MD step), to increase the probability that some MG will start providing frequency regulation services. Let t_k^+ denote the instant after the i-th MG performs the MD step at time t_k. Its share of the resource, $P_{s_i}(t_k^+)$ will decrease by the multiplicative factor β, as follows

$$P_{s_i}(t_k^+) = \beta P_{s_i}(t_k) \ . \tag{11}$$

After this phase each agent returns to the AI phase, and linearly increases its probability by a quantity α, until the next CE occurs.

Accordingly, the behavior of the i-th agent can be described by the following equation

$$P_{s_i}(t) = \beta P_{s_i}(t_k) + \alpha(t - t_k), t \in (t_k, t_{k+1}) \ , \tag{12}$$

where t_k represents one of the times instants at which the CE occurs. Note that the implementation of this simple strategy does not require the MGs to exchange information among themselves, and a single bit of communication is required to notify the MGs of CEs.

The previous algorithm can be also implemented in an *unsynchronized* version, where only a subset of the MGs perform the MD step when a CE occurs, while the others keep increasing their probability of operating in the convenient M-Mode. In this way, it is possible to take into account the different needs of single MGs, namely, their utility functions. It can be proven that the unsynchronized version of the AIMD can be used to obtain convergence of the long-term average state to the optimal point of a particular class of optimization problems, called *optimal resource allocation problems* [18]. In particular, if we consider the long-term average of the state variables $\overline{P_{si}}(t)$

$$\overline{P_{si}}(t) = \frac{1}{T}\int_0^t d\tau P_{s_i}(\tau) \ , \tag{13}$$

we can then make MG perform the MD step with probability

$$\pi_i\left(\overline{P_{si}}(t)\right) = \Gamma \frac{f_i'\left(\overline{P_{si}}(t)\right)}{\overline{P_{si}}(t)} \ , \tag{14}$$

where $f_i'(\cdot)$ denotes the derivative of the cost function while Γ is a constant ensuring that $0 \leq \pi_i(x_i) \leq 1$ for all $P_{s_i} \in i = 1, ..., n$. Equation (14) implies that each MG will react to a CE independently from the other MGs, with a customized probability $\pi_i\left(\overline{P_{si}}(t)\right)$. Then the MD step is performed on the quantity $P_{s_i}(t)$ according to (11).

Another advantage of the unsynchronized AIMD algorithm is that it can be implemented in a plug-and-play fashion: adding a new MG to the system requires no change to the existing control strategy as the algorithm will simply converge to a new equilibrium. For further details on this subject we refer the interested reader to [18] and [33]. Finally, both centralized and decentralized versions of AIMD may be implemented, depending on whether global or local frequencies are used to give rise to CEs:

- *Centralized AIMD algorithm*: The broadcast signal is provided by a central entity (e.g., a system operator). In the following, we assume that the signal is the frequency of the center of inertia (ω_{COI}).[2]
- *Decentralized AIMD algorithm*: The controllers of each MG are fully decoupled. The broadcast signal is the local frequency measured at the MG point of connection with the grid.

The main practical difference between the two strategies lies in that, during a transient, bus frequencies can be affected by local oscillation modes and noise, while ω_{COI} filters such local effects [34]. To take into account that the frequency does not vary instantaneously and that it would be unrealistic for a MG to change its active power set-point too often, the frequency boundary is reduced by a multiplicative factor $M < 1$ and the switching from F-Mode to M-Mode is allowed only at fixed event times, occurring every T_p seconds. Algorithms 1 and 2, shown below, provide the pseudo codes of two proposed versions of the AIMD algorithms. For the decentralized case, we refer to the i-th MG and the same code is executed in parallel on every MG in the transmission system. In both cases, rand(1) is used to generate a random number from a uniform distribution in $[0, 1]$, as required to practically implement Equation (14).

Algorithm 1 Centralized AIMD Algorithm

Initialization: $k = 1$, $\boldsymbol{P_s} = \mathbf{0}$;
Broadcast the parameter Γ to the entire network;
while $k < k_{\text{simulation}}$ **do**
  if $|\omega_{\text{COI}} - \omega_0| \leq M\overline{\omega}_m$ **then**
    $\boldsymbol{P_s}(k+1) = \boldsymbol{P_s}(k) + \alpha\mathbf{1}$
  else
    for $i = 1, \ldots, n$ **do**
      if $\text{rand}(1) \leq \pi_i(k) = \Gamma \frac{f_i'\left(\overline{P_{si}}(k)\right)}{\overline{P_{si}}(k)}$ **then**
        $P_{s_i}(k+1) = \beta P_{s_i}(k)$
  $k = k + 1$

Remark: It is important to emphasize that the proposed control schemes are designed to mitigate the effects of MGs

[2]Note that the frequency of a pilot bus of the system as measured by a control center of the system operator can be utilized as well.

Algorithm 2 Decentralized AIMD Algorithm

Initialization: $k = 1$, $P_{s_i} = 0$;
Broadcast the parameter Γ to the entire network;
while $k < k_{\text{simulation}}$ **do**
  if $|\omega_{B_i} - \omega_0| \leq M\overline{\omega}_m$ **then**
    $P_{si}(k+1) = P_{si}(k) + \alpha$
  else if $\text{rand}(1) \leq \pi_i(k) = \Gamma \frac{f_i'(\overline{P}_{si}(k))}{\overline{P}_{si}(k)}$ **then**
    $P_{s_i}(k+1) = \beta P_{s_i}(k)$
  $k = k + 1$

on the power grid while allowing them to maintain, at least partially, their operational freedom. However, this strategy is not suitable to quickly react to exogenous contingencies. Due to its stochastic nature, especially if the granularity of the system is not large enough,[3] the imposed boundaries on the frequency can be point-wisely violated.

IV. Case Study

This section discusses the dynamic response of a system with inclusion of MGs, regulated by means of EMSs proposed in the previous Section. The controllers are hereby compared and discussed in various simulations to evaluate their overall performance. Simulations are based on the IEEE 39-bus 10-machine system [35]; this benchmark grid is chosen to have both a fairly complex network and reduced state-space dimensions to easily understand the impact of MGs on the system.

In this case study, 12 groups of 3 MGs are connected to 12 different buses of the IEEE 39-bus. This leads to a total of 36 MGs connected to the ac system. Relevant MGs parameters are shown in Table II. In the table, the generated power $\bar{p}_g$ and the load consumption $\bar{p}_l$ refer to the average values assumed along the simulations. The values of σ_{net} are chosen randomly to take into account different variations of the load and the DERs energy production of each MG.

Four different scenarios are proposed, as follows:

S1: 36 MGs with no control system;

S2: 36 MGs with the Algorithm 1 as control system. The objective function for the i-th MG is

$$f_i(P_{s_i}) = \frac{1}{2}P_{s_i}^2 - P_{s_i} \ . \tag{15}$$

S3: 36 MGs with the Algorithm 2 as control system. The objective function for the i-th MG is

$$f_i(P_{s_i}) = \frac{1}{2}P_{s_i}^2 - P_{s_i} \ . \tag{16}$$

S4: 36 MGs with the Algorithm 2 as control system and two different objective functions. In this scenario we consider again a decentralized controller, but two different functions, $f_{i_1}(\cdot)$ and $f_{i_2}(\cdot)$ are adopted for the MGs. This scenario shows how the choice of $f_i(\cdot)$ impacts the behavior of the control system:

$$\begin{aligned} f_{i_1}(P_{s_i}) &= \frac{1}{2}P_{s_i}^2 - P_{s_i} \ , \\ f_{i_2}(P_{s_i}) &= \frac{1}{4}P_{s_i}^4 - \frac{1}{2}P_{s_i}^2 \ . \end{aligned} \tag{17}$$

[3] A thorough discussion on the impact of granularity of MGs on system dynamics is given in [14].

TABLE I: Controller parameters

Scenario	α	β	M	T_p [s]	Γ
S2	0.015	0.95	0.9	30	-1
S3	0.015	0.95	0.9	30	-1
S4	0.015	0.95	0.9	30	-1

Also, all objective functions above have their minimum in $P_{s_i} = 1$ (given the domain $[0, 1]$) which fits the interpretation of each MG trying to maximize the time spent in M-Mode instead of regulating the frequency.

In Subsection IV-B the deviations of the frequency of the third scenario obtained with the decentralized AIMD as control system are compared with the ones obtained with a PI-based controller in order to show the effectiveness of the strategy proposed in this paper with respect to a simpler methodology. The interested reader can refer to [16] for a detailed discussion about the performance of the PI-based controller.

The state-space of the each case with 36 MG includes 432 state variables and 848 algebraic ones. The results for each scenario are obtained based on a Monte Carlo method (all the simulations are solved for each scenario). All simulations are solved using Dome, a Python-based software tool for power system analysis [36].

In all scenarios above, ω_0 and $\overline{\omega}_m$ are set. respectively to 1 and 0.02 pu. Table I shows the controller parameters employed in these simulations. The value of Γ is chosen in such a way to make sure that $\pi_i(k)$ belong to the interval $[0, 1]$.

The performance of the controllers is evaluated considering the maximum among the infinity norms of the local frequencies, according to

$$||\boldsymbol{\omega}||_\infty(t) = \max\{||\omega_i(t)||_\infty, i \in \Theta\} \ , \tag{18}$$

and comparing the average of the switching probabilities $P_{s_i}(t)$, over time, according to

$$\overline{\boldsymbol{P_s}}(t) = \frac{1}{n}\sum_{i=1}^{n} P_{s_i}(t) \ . \tag{19}$$

A. Simulations Results

Figures 2a to 2d and 3a to 3f show the realizations of the bus frequencies, the realizations of the switching probabilities and their averages, computed according to (19), in the proposed scenarios. Results shows that, for S1, frequency oscillations are inadequate for the operation of the transmission system. On the other hand, Figs. 2b to 2d show that the unsynchronized AIMD utilized in S2-S4 mitigates the frequencies oscillations bringing them within (or at least very close to) the desired security band.

Table III and Figures 2b, 2c and 3c, 3d compare the performances of the centralized and the decentralized controllers. We observe that, despite $\overline{\boldsymbol{P_s}}(t)$ presents larger values

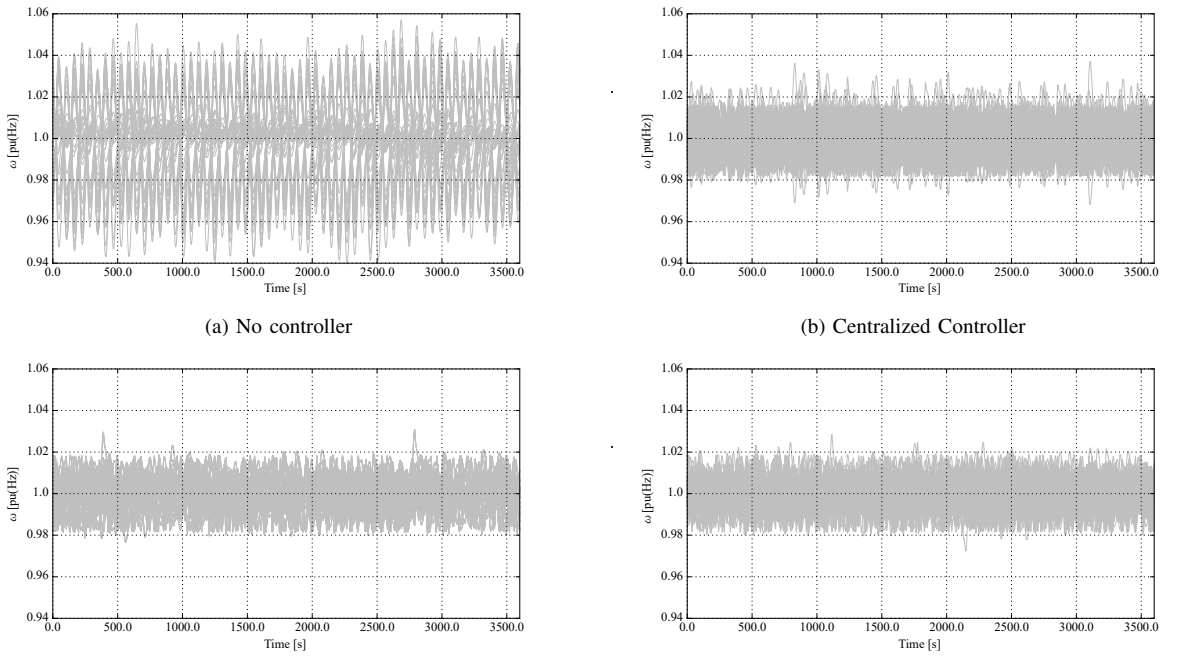

(a) No controller

(b) Centralized Controller

(c) Decentralized Controller

(d) Decentralized Controller with different objective functions

Fig. 2: Frequency trajectories, over all the realizations, of the 39 bus system.

TABLE II: Microgrid parameters

MG	Bus	$\bar{p}_g$ [pu(MW)]	$\bar{p}_l$ [pu(MW)]	σ_{net} [pu(Hz)]	T_s [s]
1	18	0.88	0.54	0.025	18000.0
2	3	0.77	0.20	0.040	25200.0
3	15	0.80	0.10	0.030	23400.0
4	17	0.40	0.20	0.020	28800.0
5	21	0.20	0.10	0.013	18000.0
6	28	0.20	0.40	0.040	25200.0
7	24	0.36	0.84	0.010	23400.0
8	17	0.20	0.50	0.020	28800.0
9	11	0.20	0.30	0.010	14400.0
10	5	0.10	0.80	0.010	18000.0
11	7	0.80	0.10	0.030	26640.0
12	12	0.40	0.40	0.025	24480.0

TABLE III: Controller performance

Scenario	$\|\|\boldsymbol{\omega}\|\|_\infty$ (pu Hz)
S1	1.060
S2	1.038
S3	1.028
S4	1.025

overall in S2 (see Figures 3a and 3b), the realizations of the frequency oscillate outside the desired range more often in the S2 (centralized controller) than in S3 (decentralized controller) (see Figures 2b and 2c). Moreover, the frequencies reach higher values with the centralized controller.

The rationale behind this is that, since in the S2 the CEs are triggered by the ω_{COI}, the controller neglects local frequency variations and, therefore, grants more operational freedom to each MG. On the other hand, in S3, the decentralized controller is able to keep each frequency within the operational boundaries since CEs are triggered by local frequencies. This implies that the decentralized controller behaves less conservatively than the centralized one and therefore MGs are forced to employ more active power for primary frequency regulation.

A further element of comparison are the P_{s_i} of each MG. Fig. 3c and 3d show the switching probabilities P_{s_i} of each MG averaged across all the realizations. In S2, the numerical differences among the probabilities are very small when compared to the third one, in which the P_{s_i} values are very different among MGs. Again, this difference is caused by the different control signals employed: in fact since in the third scenario the CEs are triggered by variations of the local frequencies ω_{B_i}, some MGs might have to regulate the frequency more often due to their geographical position – e.g., they might be close to a very sensitive synchronous machine and therefore they enter the MD step more often than others.

The discussion above suggests a drawback in the decentralized approach: it inherently makes the control mechanism unfair, penalizing some agents and rewarding others on the basis of their geographical position. To solve this issue and to analyze the impact of different objective functions, in S4, the 36 MGs are divided into two groups of 18 MGs each. A group is characterized by a penalizing cost function ($f_{i_1}(\cdot)$), while the other one is characterized by a rewarding cost function ($f_{i_2}(\cdot)$). The effects of this choice are shown in Figures 2d, 3e and 3f and Table III. The frequency lies within the boundaries imposed by $\overline{\omega}_m$ and the penalized group of MGs (Fig. 3e) has a smaller $\overline{\boldsymbol{P_s}}(t)$ with respect to the rewarded one (Fig. 3f).

The overall $\overline{\boldsymbol{P_s}}(t)$ does not change with different choices of the $f_i(\cdot)$. This means that, changing the objective functions

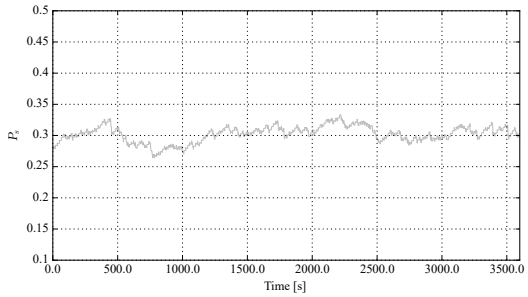

(a) Average $\overline{\boldsymbol{P_s}}(t)$, over all the realizations, of the centralized controller

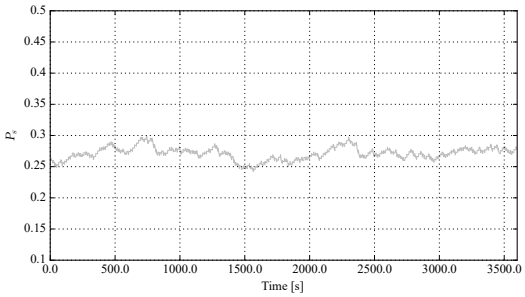

(b) Average $\overline{\boldsymbol{P_s}}(t)$, over all the realizations, of the decentralized controller

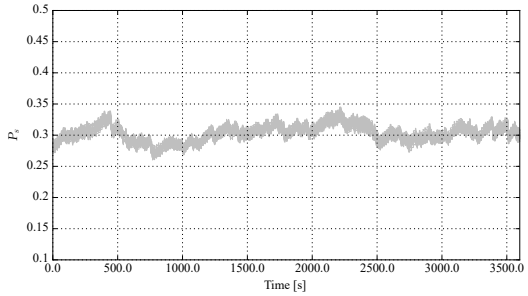

(c) All $P_{s_i}(t)$ trajectories , over all the realizations, of each MG for the centralized controller

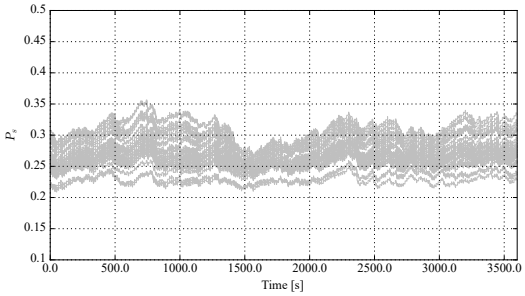

(d) All $P_{s_i}(t)$ trajectories, over all the realizations, of each MG for the decentralized controller

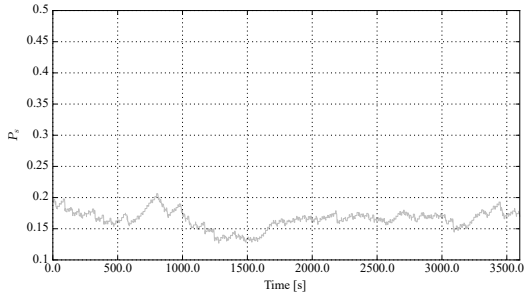

(e) Average $\overline{\boldsymbol{P_s}}(t)$, over all the realizations, with the penalizing objective function

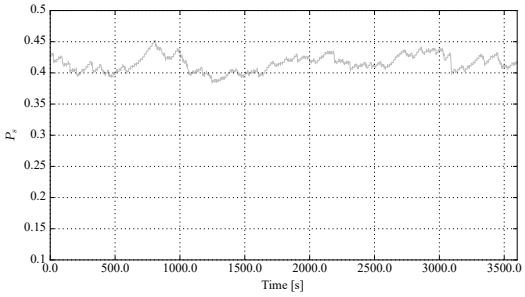

(f) Average $\overline{\boldsymbol{P_s}}(t)$, over all the realizations, with the rewarding objective function

Fig. 3: Plots of the switching probabilities, averaged across all the realizations of the stochastic processes.

does not alter the overall performance of the controller but it forces some agents to provide more ancillary services than others. The utilization of different cost functions could then be used to fix the fairness issue in the decentralized approach or to reward or penalize the energy policies of the MGs participating in the frequency regulation, e.g., a MG might be rewarded with a lower regulation burden due to its low CO_2 emissions.

Overall, the decentralized approach, which requires almost no communication among agents and has a robust architecture, provides better performance than the centralized controller. The decentralized controller is, in fact, able to provide a fair and adequate regulation of all the frequencies of the system (the fairness can obtained through the tuning of the objective functions $f_i(\cdot)$), whereas the centralized one, despite being intrinsically fair, provides worse performance in terms of regulation.

B. Comparison between the AIMD and a PI-based controller

In order to show the effectiveness of the AIMD, we hereby compare the performances of the control strategy proposed in this paper with the control strategy proposed in [16]. In [16], the authors employed a PI-based controller to regulate the switching between the M-Mode and the F-Mode, that is based on the current and previous values of the standard deviation of the frequency.

The probability P_{s_i} of the i-th MG is computed as follows. Every T_{p_i} seconds, the controller updates P_{s_i} to operate in F-Mode in the next time window. The quantity $P_{s_i}(kT_{p_i})$, at the k-th time window, is computed as

$$P_{s_i}(kT_{p_i}) = \frac{3\left[\gamma\sigma_h(kT_{p_i}) + (1-\gamma)\sum\limits_{n=k-L}^{k-1} l_n\sigma_h(nT_{p_i})\right]}{\overline{\omega}_m}, \tag{20}$$

where $\sigma_h(kT_{p_i})$ is the standard deviation of the frequency

at the h-th bus (to which the i-th MG is connected) in the time window $[(k-1)T_{p_i}, kT_{p_i}]$; γ is a parameter belonging to $[0, 1]$; L represents the number of past values of σ_{COI} that are taken in consideration; and l_n are positive coefficients chosen such that $\sum_{n=1}^{L-1} l_n = 1$. This control law resembles a discrete PI controller, as it takes into account the actual value of the controlled variable σ_{COI} and its weighted integral.

Figure 4 shows the frequencies of the IEEE 39 bus with the two approaches: it is clear by visual inspection that, despite both controllers manage to keep the frequency bounded, the PI-based control forces the MG to regulate the frequency in a narrower interval, meaning that the average number of switchings is greater than that obtained with the AIMD control strategy. This implies that the MG regulated through the PI-based control are operated in M-Mode during an overall smaller time than the MG regulated with the AIMD approach, and thus achieve a lower revenue.

In terms of the optimization problem (10) this means that the variables $\boldsymbol{P_s(t)}$ obtained with the PI-based approach are larger than the variables $\boldsymbol{P_s(t)}$ obtained with the AIMD strategy. The second controller is therefore able to provide a better solution to (10), with respect to the one provided by the PI-based approach.

V. Conclusions

This work proposes an application of the unsynchronized (decentralized) AIMD algorithm to mitigate the negative impact on the power system of a large number of MGs that manage their internal power flow according to their own policy.

The main conclusion of the paper is that a large number of MGs are able to adopt aggressive policies (e.g., maximizing their revenues trying to exploit the energy market) as long as they provide ancillary services, in the form of primary regulation, to maintain the frequency stability of the transmission system. The unsynchronized AIMD algorithm appears to be an excellent candidate to achieve this trade off due to its robustness and ability to maintain the system frequency within the operational boundaries with a decentralized architecture.

Simulations show that a decentralized approach is able to reduce the fluctuations of the frequency in the desired range while a centralized strategy fails to achieve the same results. Moreover, proper tuning of the objective functions assigned to each MG allow to obtain fairness (i.e., each MG will provide the same amount of frequency regulation on average) or to promote different policies among the MGs, through the use of penalizing and rewarding functions.

References

[1] C. Dou, M. Lv, T. Zhao, Y. Ji and H. Li, *Decentralised coordinated control of microgrid based on multi-agent system*, IEEE Generation, Transmission and Distribution, Vol. 9, No. 16, pp. 2474-2484, 2015.

[2] A. Nisar and M. S. Thomas, *Comprehensive Control for Microgrid Autonomous Operation With Demand Response*, IEEE Trans. on Smart Grid, Vol. 8, No. 5, pp. 2081-2089, 2016.

[3] J. P. Guerrero, J. C. Vásquez, J. Matas, L. García de Vicuna, M. Castilla, *Hierarchical Control of Droop-Controlled AC and DC Microgrids – A General Approach Toward Standardization*, IEEE Trans. on Industrial Electronics, Vol. 58, No. 1, pp. 158-172, 2010.

[4] H. Asano, N. Hatziargyriou, R. Iravani, and C. Marnay, *Microgrids: an overview of ongoing research, development, and demonstration projects* IEEE Power Energy Magazine, Vol. 6, No. 3, pp. 78-94, 2008.

[5] G. Carpinelli, F. Mottola, D. Proto and A. Russo, *A Multi-Objective Approach for Microgrid Scheduling*, IEEE Trans. on Smart Grid, Vol. 8, No. 5, pp. 2109-2118, 2017.

[6] A. R. Malekpour and A. Pahwa, *Stochastic Networked Microgrid Energy Management With Correlated Wind Generators*, IEEE Trans. on Power Systems, Vol. 32, No. 5, pp. 3681-3693, 2017.

[7] W. J. Ma, J. Wang, X. Lu and V. Gupta, *Optimal Operation Mode Selection for a DC Microgrid*, IEEE Trans. on Smart Grid, Vol. 7, No. 6, pp. 2624-2632, 2016.

[8] Z. Shuai, Y. Hu, Y. Peng, C. Tu and Z. J. Shen, *Dynamic Stability Analysis of Synchronverter-Dominated Microgrid Based on Bifurcation Theory*, IEEE Trans. on Industrial Electronics, Vol. 64, No. 9, pp. 7467-7477, 2017.

[9] Z. Zhao, P. Yang, J. M. Guerrero, Z. Xu and T. C. Green, *Multiple-Time-Scales Hierarchical Frequency Stability Control Strategy of Medium-Voltage Isolated Microgrid*, IEEE Trans. on Power Electronics, Vol. 31, No. 8, pp. 5974-5991, 2016.

[10] J. Schiffer, T. Seel, J. Raisch and T. Sezi, *Voltage Stability and Reactive Power Sharing in Inverter-Based Microgrids With Consensus-Based Distributed Voltage Control*, IEEE Trans. on Control Systems Technology, Vol. 24, No. 1, pp. 96-109, 2016.

[11] A. Ulbig, T. S. Borsche, and G. Andersson, *Impact of Low Rotational Inertia on Power System Stability and Operation*, IFAC, Vol. 47, pp. 7290-7297, 2014.

[12] J. Zhang, S. Su, J. Chen, and F. Hong, *Stability Analysis of the Power System with the Large Penetration Ratios of Microgrids*, SUPERGEN, pp. 1-5, 2009.

[13] H. Golpira, H. Seifi, A. R. Messina and Mahmoud-Reza Haghifam, *Maximum Penetration Level of Micro-Grids in Large-Scale Power Systems: Frequency Stability Viewpoint*, IEEE Trans. on Power Systems, Vol. 31, No. 6, pp. 5163-5171, 2016.

[14] P. Ferraro, E. Crisostomi, M. Raugi and F. Milano, *Analysis of the Impact of Microgrid Penetration on Power System Dynamics*, IEEE Trans. on Power Systems, Vol. 32, No. 5, pp. 4101-4109, 2017.

[15] P. Ferraro, E. Crisostomi, M. Raugi and F. Milano, *On the Impact of Microgrid Energy Management Systems on Power System Dynamics*, IEEE PES General Meeting, pp. 1-5, 2017.

[16] P. Ferraro, E. Crisostomi, M. Raugi and F. Milano, *Decentralized Stochastic Control of Microgrids to Improve System Frequency Stability*, IEEE ISGT Europe, pp. 1-6, 2017.

[17] S.H. Tindemans, V. Trovato and G. Strbac, *Decentralized Control of Thermostatic Loads for Flexible Demand Response*, IEEE Trans. on Control Systems Technology, Vol. 23, No. 5, pp. 1685-1700, 2015.

[18] W. Griggs, J.Y. Yu, F. Wirth, F. Hauesler and R. Shorten *On the design of campus parking systems with QoS guarantees*, IEEE Trans. on Intelligent Transportation Systems, Vol. 17, No. 5, pp. 1428-1437, 2016.

[19] D.Angeli and P.A. Kountouriotis, *A stochastic approach to dynamic-demand refrigerator control*, IEEE Trans. on Control System Technology, Vol. 20, No. 3, pp. 581-592, 2012.

[20] Q. Shafiee, J. C. Vásquez, and J. M. Guerrero. *A Distributed Secondary Control for Islanded MicroGrids. A Networked Control Systems Approach*, IECON pp. 5637-5642, 2012.

[21] N. Pogaku, M. Prodanović and T. C. Green., *Modeling, Analysis and Testing of Autonomous Operation of an Inverter-Based Microgrid*, IEEE Trans. on Power Electronics, Vol. 22, No. 2, pp. 613-625, 2007.

[22] I. A. Hiskens, *Power System Modeling for Inverse Problems*, IEEE Trans. on Circuits and Systems I: Regular Papers, Vol. 51, No. 3, pp. 539-551, 2004.

[23] F. Milano, *Power System Modelling and Scripting*, Springer, London, 2010.

[24] F. L. Alvarado, J. Meng , C. L. DeMarco and W. S. Mota, *Stability Analysis of Interconnected Power Systems Coupled with Market Dynamics*, IEEE Trans. on Power Systems, Vol. 16, No. 4, pp. 695-701, 2001.

[25] Wei-Yu Chiu, H. Sun, and H. V. Poor, *A Multiobjective Approach to Multimicrogrid System Design*, IEEE Trans. on Smart Grid, Vol. 6, No. 5, pp. 2263-2272, 2015.

[26] B. Tamimi, C. Cañizares and K. Bhattacharya, *Modeling and Performance Analysis of Large Solar Photo-Voltaic Generation on Voltage Stability and Inter-area Oscillations*, IEEE PES General Meeting, pp. 1-6, 2011.

[27] F. Milano, *Control and Stability of Future Transmission Networks*, in *The Handbook of Clean Energy Systems - Volume 4*, editor Prof. Jinyue Yan, John Wiley & Sons, 2015.

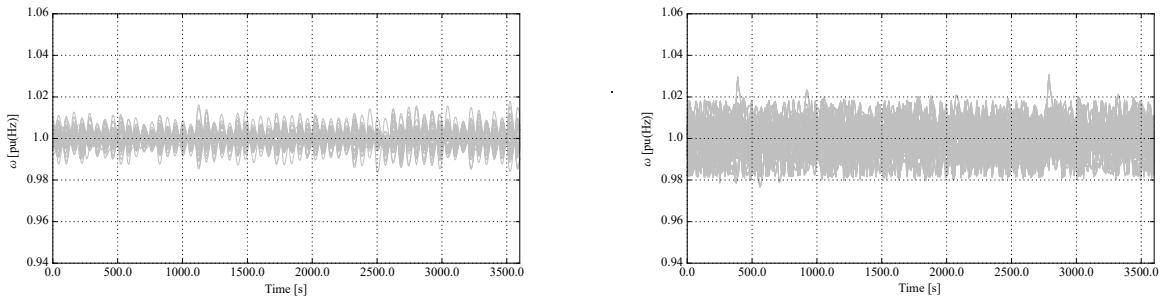

(a) PI-based controller

(b) Decentralized AIMD Controller

Fig. 4: Frequency trajectories, over all the realizations, of the 39 bus system with two different switching strategies.

[28] F. Milano and R. Zárate-Miñano, *A Systematic Method to Model Power Systems as Stochastic Differential Algebraic Equations*, IEEE Trans. on Power Systems, vol. 28, no. 4, pp. 4537-4544, Nov. 2013.

[29] C. Roberts, E. M. Stewart, F. Milano, *Validation of the Ornstein-Uhlenbeck Process for Load Modeling Based on μPMU Measurements*, PSCC, pp. 1-7, 2016.

[30] F. Milano and Á. Ortega, *Frequency Divider*, IEEE Trans. on Power Systems, Vol. 32, No. 2, pp. 1493-1501, 2017.

[31] F. Baccino, F. Conte, S. Massucco, F. Silvestro and S. Grillo, *Frequency regulation by management of building cooling systems through Model Predictive Control*, PSCC, pp. 1-7, 2014.

[32] P. Kundur, *Power System Stability and Control*, McGraw-Hill, 1994.

[33] M. Corless, C. King, R. Shorten, and F. Wirth, *AIMD Dynamics and Distributed Resource Allocation*, SIAM, 2015.

[34] Á. Ortega, F. Milano, *Comparison of Bus Frequency Estimators for Power System Transient Stability Analysis*, POWERCON, pp. 1-6, 2016.

[35] Illinois Center for a Smarter Electric Grid (ICSEG), *IEEE 39-Bus System*, available at: http://publish.illinois.edu/smartergrid/ieee-39-bus-system/.

[36] F. Milano, *A Python-based Software Tool for Power System Analysis*, IEEE PES General Meeting, pp. 1-5, 2013.

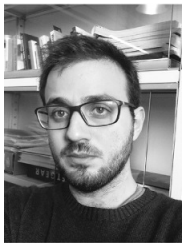

Pietro Ferraro received the M.Sc. degree in automatics and robotics from the University of Pisa, Italy, in 2014. He is currently a Ph.D. candidate with the Department of Energy, Systems, Territory and Constructions Engineering, University of Pisa. His research interests include control theory, optimization and time series analysis, with application to smart grids.

Emanuele Crisostomi received the B.Sc. degree in computer science engineering, the M.Sc. degree in automatic control, and the Ph.D. degree in automatics, robotics, and bioengineering, from the Univ. of Pisa, Italy, in 2002, 2005, and 2009, respectively. He is currently an Assistant Professor of electrical engineering with the Department of Energy, Systems, Territory and Constructions Engineering, Univ. of Pisa. His research interests include control and optimization of large scale systems, with applications to smart grids and green mobility networks.

Robert Shorten Robert N. Shorten received the B.E. degree in electronic engineering and the Ph.D. degree from the University College Dublin (UCD), Dublin, Ireland, in 1990 and 1996, respectively. From 1993 to 1996, he was the holder of a Marie Curie Fellowship and employee at Daimler-Benz Research, Berlin, Germany, to conduct research in the area of smart gearbox systems. Following a brief spell at the Center for Systems Science, Yale University, working with Prof. K. S. Narendra, he returned to Ireland as the holder of a European Presidency Fellowship in 1997. He is a co-founder of the Hamilton Institute, National University of Ireland, Maynooth, Ireland, where he was a Full Professor until March 2013. He was also a Visiting Professor at the Technical University of Berlin from 2011 to 2012. From 2013-2015 he led the Control and Optimization team at IBM Research in Dublin. He is currently jointly employed by IBM Research and as a Professor of Control Engineering and Decision Science at University College Dublin. His research spans a number of areas. He has been active in computer networking, automotive research, collaborative mobility (including smart transportation and electric vehicles), as well as basic control theory and linear algebra. His main field of theoretical research has been the study of hybrid dynamical systems.

Federico Milano (S'02, M'04, SM'09, F'16) received from the University of Genoa, Italy, the ME and Ph.D. in Electrical Engineering in 1999 and 2003, respectively. From 2001 to 2002 he was with the University of Waterloo, Canada, as a Visiting Scholar. From 2003 to 2013, he was with the University of Castilla-La Mancha, Spain. In 2013, he joined the University College Dublin, Ireland, where he is currently Professor of Power Systems Control and Protections and Head of Electrical Engineering. His research interests include power system modeling, control, stability analysis ans simulation.